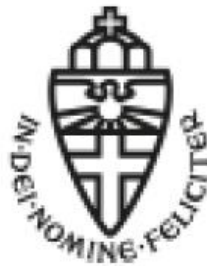


Radboud Universiteit



GRAPHENE FLAGSHIP

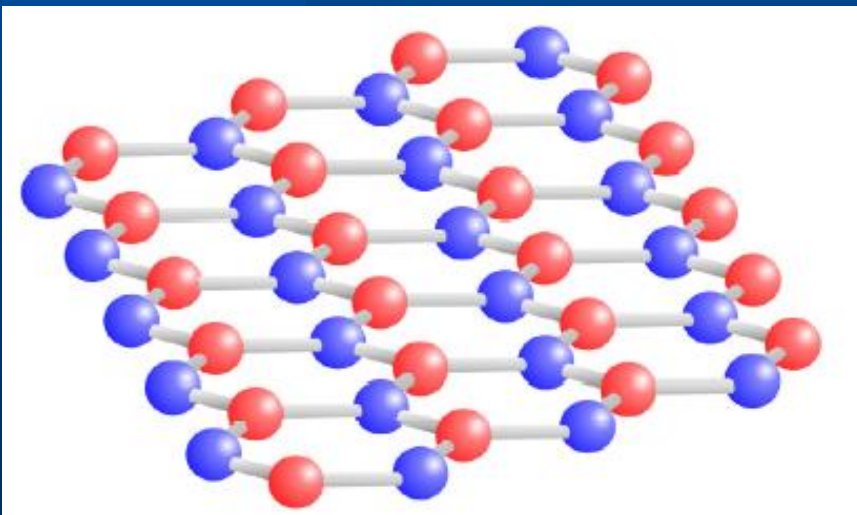
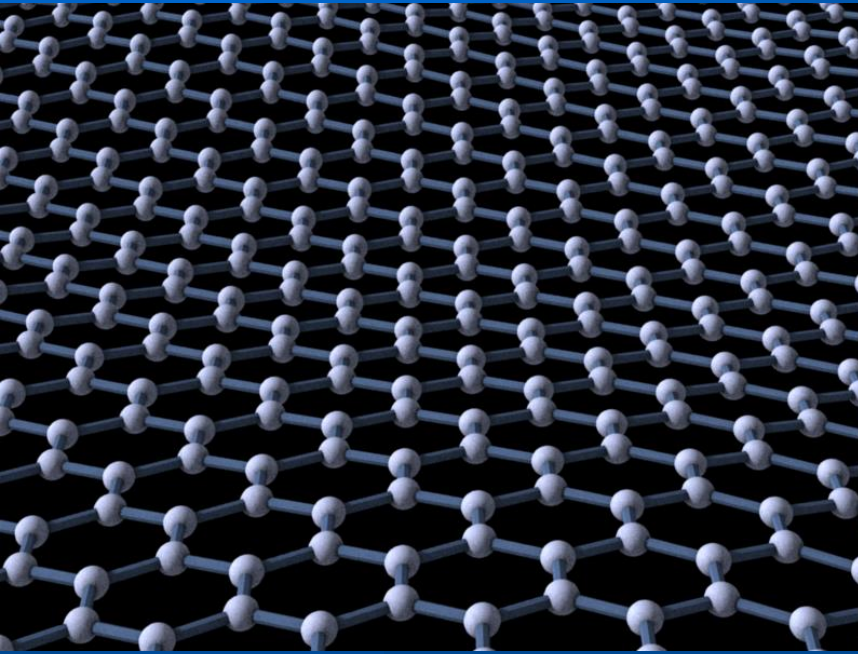


Topological and Geometric Plots in the Physics of Graphene

Mikhail Katsnelson

In collaboration with Timur Tudorovskiy,
Misha Titov, and Vladimir Nazaikinskii

Honeycomb lattice (graphene)



Two equivalent sublattices,
A and B (pseudospin)

Massless Dirac fermions in graphene

$$H = -i\hbar c^* \begin{pmatrix} 0 & \frac{\partial}{\partial x} - i \frac{\partial}{\partial y} \\ \frac{\partial}{\partial x} + i \frac{\partial}{\partial y} & 0 \end{pmatrix} \quad \hbar c^* = \frac{\sqrt{3}}{2} \gamma_0 a$$

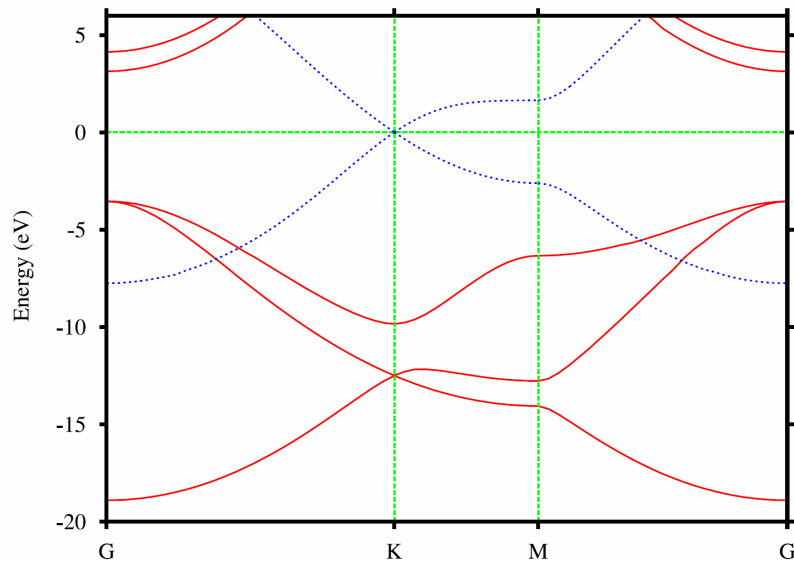
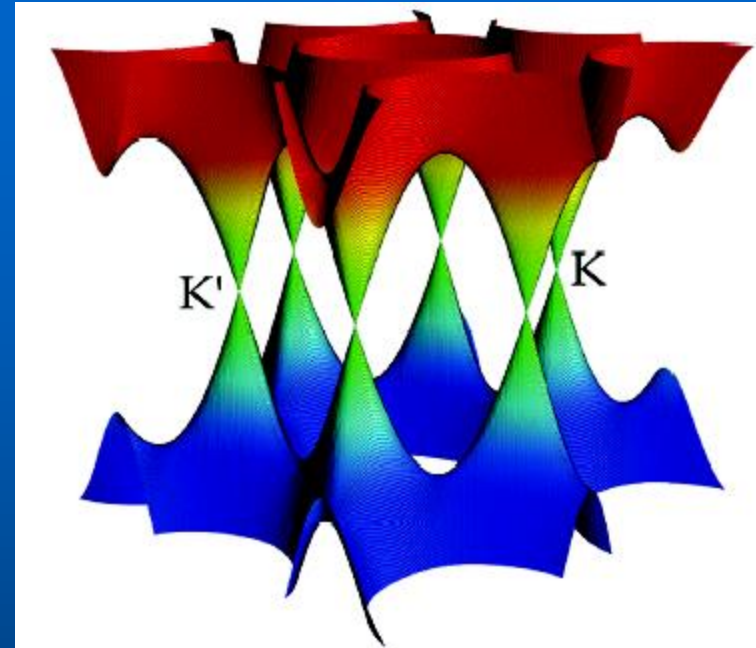


FIG. 2: (color online) Band structure of a single graphene layer. Solid red lines are σ bands and dotted blue lines are π bands.



sp^2 hybridization, π bands crossing the neutrality point

Neglecting intervalley scattering:
massless Dirac fermions

Symmetry protected (T and I)

Effective Hamiltonian in magnetic field: Peierls

$$H = \frac{\hat{\pi}^2}{2m} + V(\vec{r})$$

$$\hat{\pi} = \hat{p} - \frac{e}{c} \vec{A},$$

$$\vec{p} = -i\hbar \vec{\nabla}$$

$$\vec{B} = \vec{\nabla} \times \vec{A},$$

$V(\vec{r})$ is a periodic crystal potential

$$[\hat{\pi}_x, \hat{\pi}_y] = -[\hat{\pi}_y, \hat{\pi}_x] = \frac{ie}{\hbar c} B$$

Exact formulation

Simplifications:

$$l_B \gg a$$

up to 10,000 T – OK!

$$l_B = \sqrt{\frac{\hbar c}{|e|B}}$$

magnetic length

Effective Hamiltonian in magnetic field: Peierls

$$H = \frac{\hat{\pi}^2}{2m} + V(\vec{r})$$

$$\hat{\pi} = \hat{p} - \frac{e}{c} \vec{A},$$

$$\vec{p} = -i\hbar \vec{\nabla}$$

$$\vec{B} = \vec{\nabla} \times \vec{A},$$

$V(\vec{r})$ is a periodic crystal potential

$$[\hat{\pi}_x, \hat{\pi}_y] = -[\hat{\pi}_y, \hat{\pi}_x] = \frac{ie}{\hbar c} B$$

Exact formulation

Simplifications:

$$l_B \gg a$$

up to 10,000 T – OK!

$$l_B = \sqrt{\frac{\hbar c}{|e|B}}$$

magnetic length

Solution

$$\begin{aligned}\hat{b}\psi_2 &= \varepsilon\psi_1 \\ \hat{b}^+\psi_1 &= \varepsilon\psi_2\end{aligned}$$

$$E = \sqrt{\frac{2|e|\hbar B v^2}{c}} \varepsilon \equiv \frac{\sqrt{2}\hbar v}{l_B} \varepsilon$$

Zero-energy solution:

$$\psi_1 = 0$$

$$\psi_2 \equiv |0\rangle$$

$$b|0\rangle = 0$$

Complete spectrum:

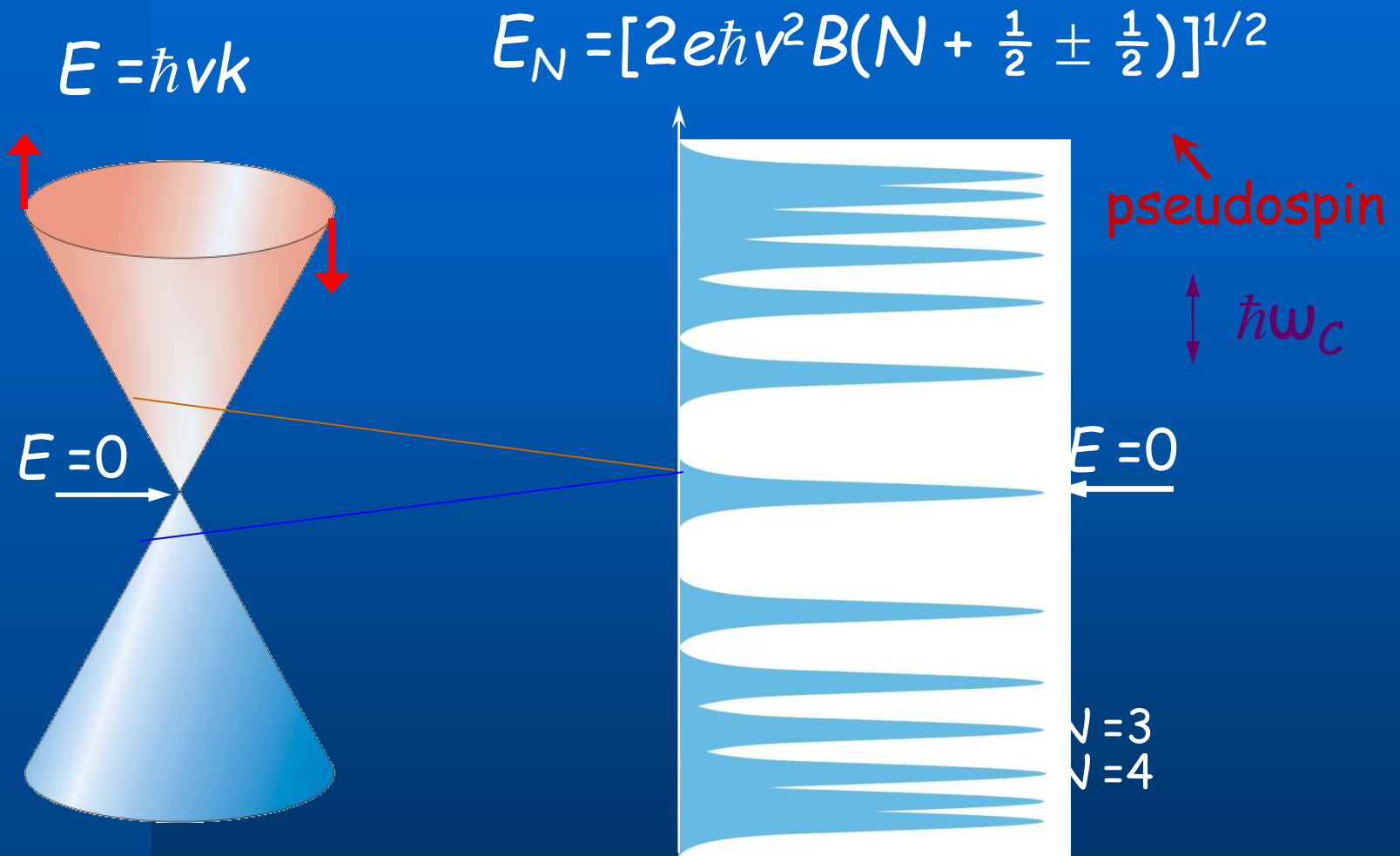
$$\hat{b}^+\hat{b}\psi_2 = \varepsilon^2\psi_2$$

$$\varepsilon_v^2 = v = 0, 1, 2, \dots$$

$$E_v^{(\pm)} = \pm \hbar \omega_c \sqrt{v}$$

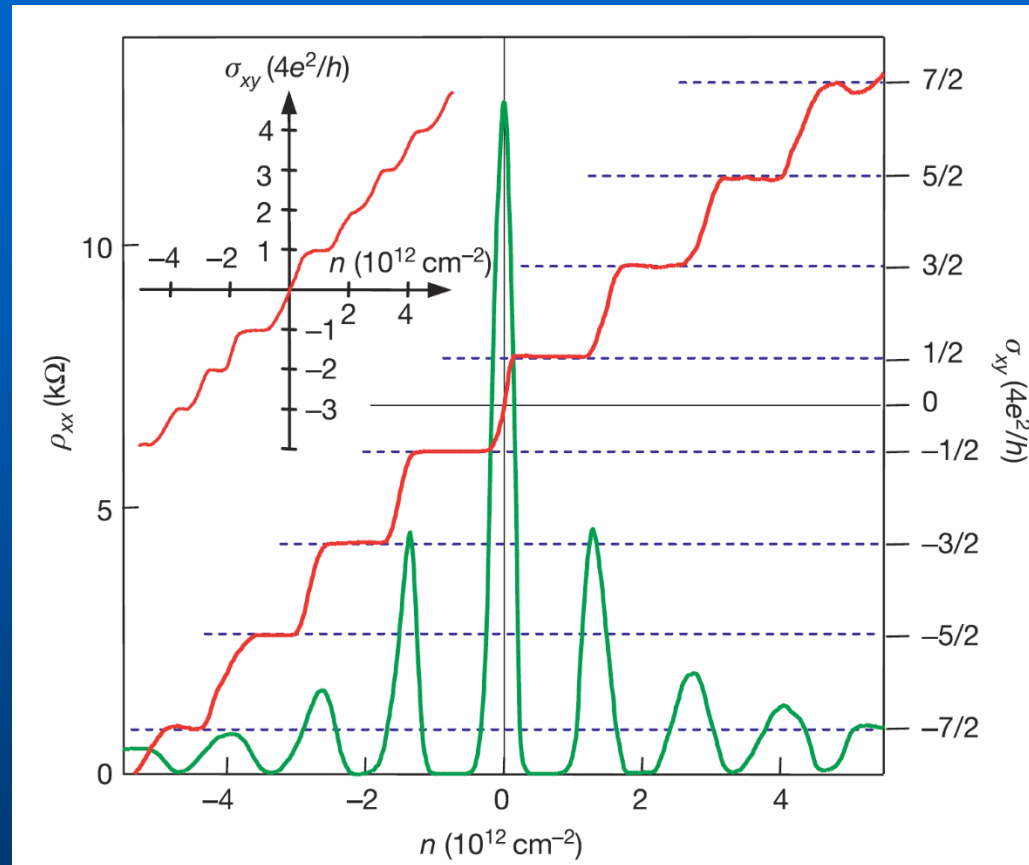
$$\hbar \omega_c = \frac{\sqrt{2}\hbar v}{l_B} = \sqrt{\frac{2\hbar|e|Bv^2}{c}}$$

Anomalous Quantum Hall Effect



The lowest Landau level is *at ZERO energy* and shared equally by electrons and holes (McClure 1956)

Anomalous QHE in single-layer graphene



Single-layer: half-integer quantization since zero-energy Landau level is equally shared by electrons and holes (Novoselov et al 2005, Zhang et al 2005)

Quantum capacitance measurements

Yu et al, PNAS 2013

Graphene on hBN: one can see many-body effects etc.

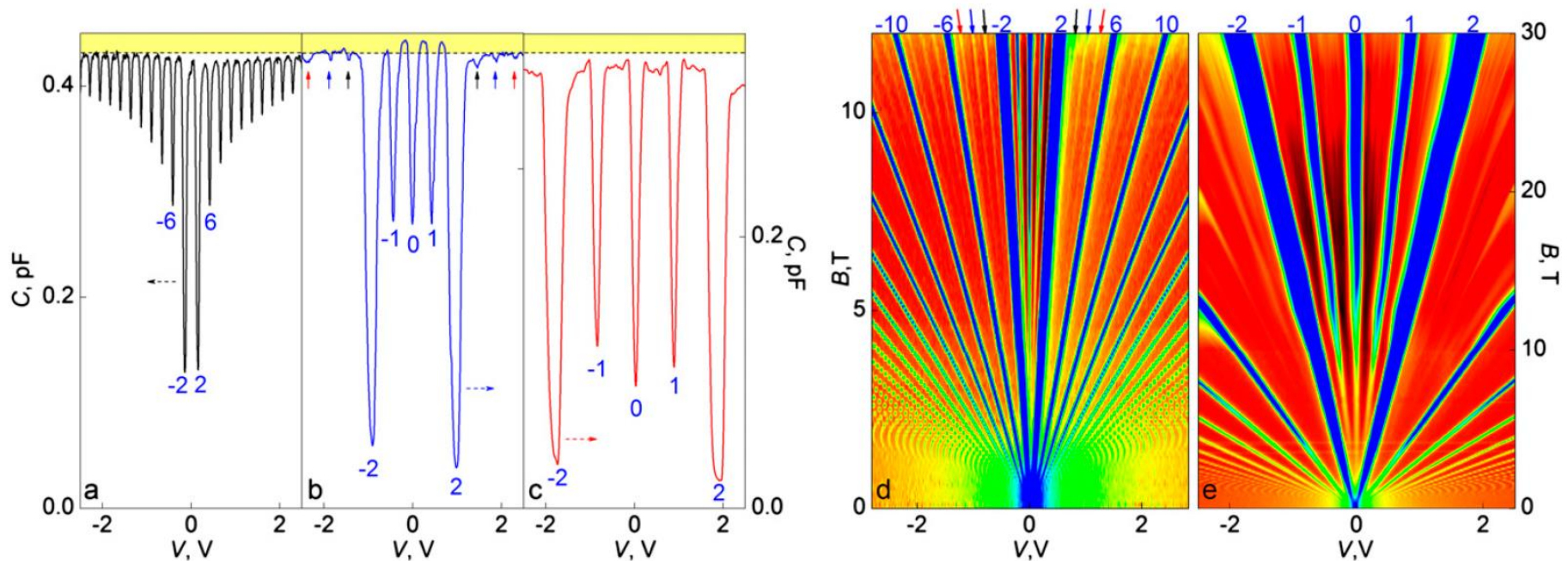


Fig. 3. Graphene capacitors in quantizing fields. (A–C) Examples of graphene capacitance for $B = 3, 15$, and 30 T, respectively. Blue numbers are ν for the corresponding minima. The arrows in B mark $\nu = \pm 3$ (black arrows), ± 4 (blue) and ± 5 (red). The dashed line indicates $C_G = 0.433 \pm 0.002$ pF (for a device shown in A) and 0.335 ± 0.002 pF (for a device shown in B and C). The 15-T curve reveals that the total capacitance becomes higher than the geometrical one at ν around $\pm 1/2$ and $\pm 3/2$, indicating a negative contribution from C_Q , that is, negative compressibility. (D) Two-dimensional map of differential capacitance as a function of B and V for the same device as in A. Color scale is 0.37 pF to C_G (blue to green to red) and C_G to 0.454 pF (red to black). Numbers and arrows are as in B. (E) Two-dimensional map in B up to 30 T for the device in B and C. Scale: 0.23 pF to C_G (blue to green to red) and C_G to 0.349 pF (red to black). The dark regions (D and E) correspond to negative C_Q .

Half-integer quantum Hall effect and “index theorem”

Atiyah-Singer index theorem: number of chiral
modes with zero energy for massless Dirac
fermions with gauge fields

Simplest case: 2D, electromagnetic field

$$N_+ - N_- = \phi / \phi_0$$

(magnetic flux in units of the flux quantum)

Magnetic field can be inhomogeneous!!!

Zero-mass lines: motivation (Graphene on hBN)

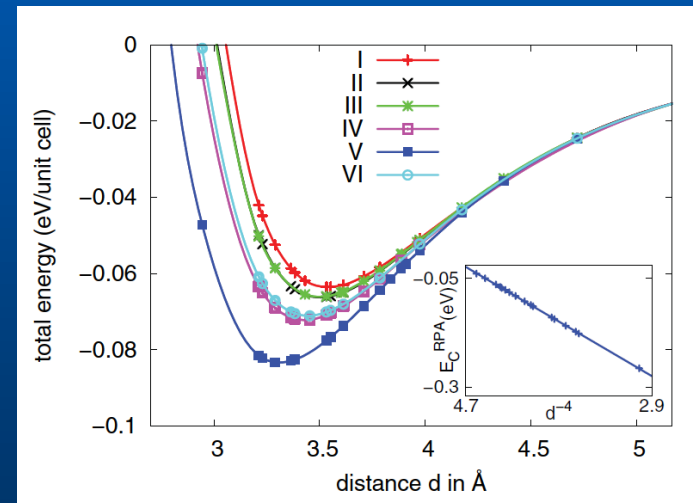
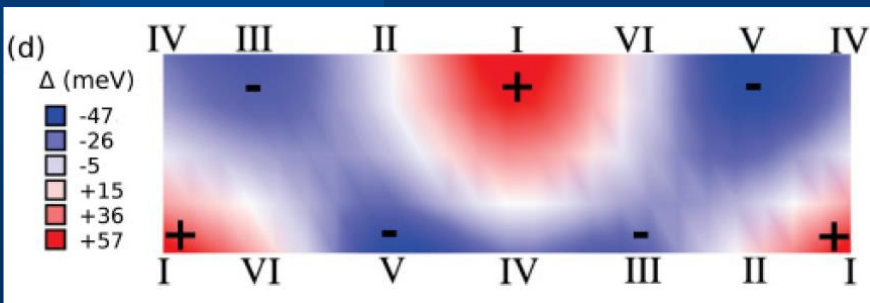
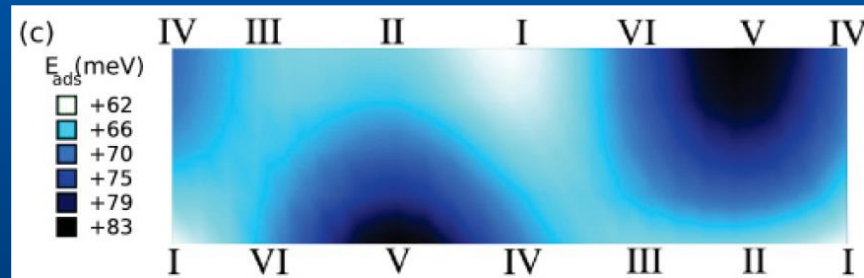
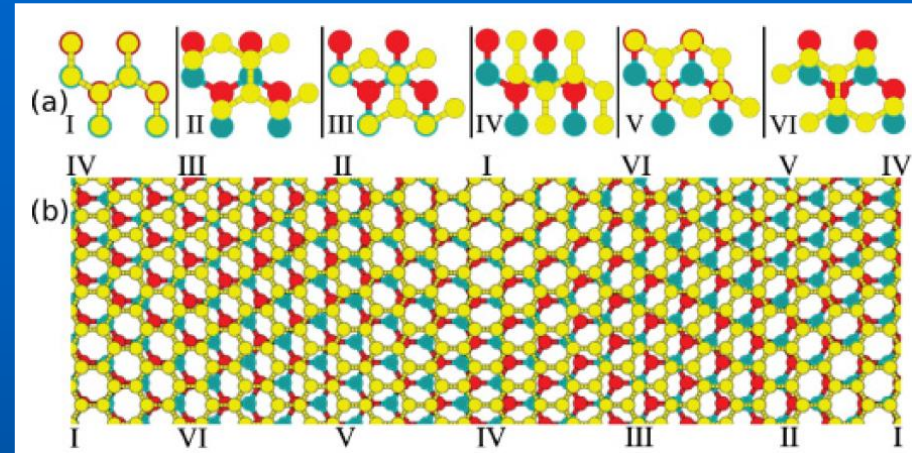
PHYSICAL REVIEW B **84**, 195414 (2011)

Adhesion and electronic structure of graphene on hexagonal boron nitride substrates

B. Sachs,^{1,*} T. O. Wehling,^{1,†} M. I. Katsnelson,² and A. I. Lichtenstein¹

Relaxed structure (B green, C yellow, N red)

V corresponds to the minimal energy (max. cohesion)



B on the top of C, N in the middle of hexagon
Sublattices are no more equivalent \rightarrow locally energy gap is open (mass term in Dirac eq.)

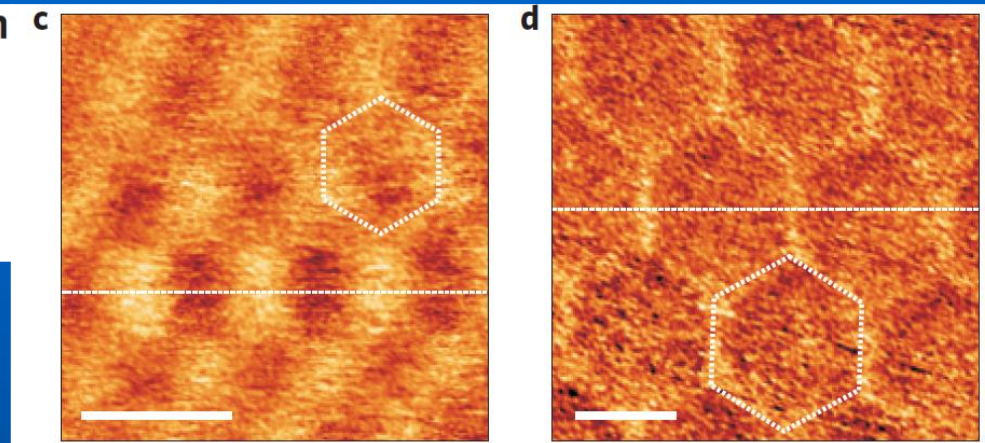
Commensurate-incommensurate transition

Commensurate-incommensurate transition in graphene on hexagonal boron nitride

C. R. Woods¹, L. Britnell¹, A. Eckmann², R. S. Ma³, J. C. Lu³, H. M. Guo³, X. Lin³, G. L. Yu¹, Y. Cao⁴, R. V. Gorbachev⁴, A. V. Kretinin¹, J. Park^{1,5}, L. A. Ponomarenko¹, M. I. Katsnelson⁶, Yu. N. Gornostyrev⁷, K. Watanabe⁸, T. Taniguchi⁸, C. Casiraghi², H.-J. Gao³, A. K. Geim⁴ and K. S. Novoselov^{1*}

NATURE PHYSICS DOI: 10.1038/NPHYS2954

When misorientation angle (in radians) is smaller with misfit, synchronization happens



Moiré patterns with periodicity 8 nm (left) and 14 nm (right)

Atomistic simulations

PRL **113**, 135504 (2014)

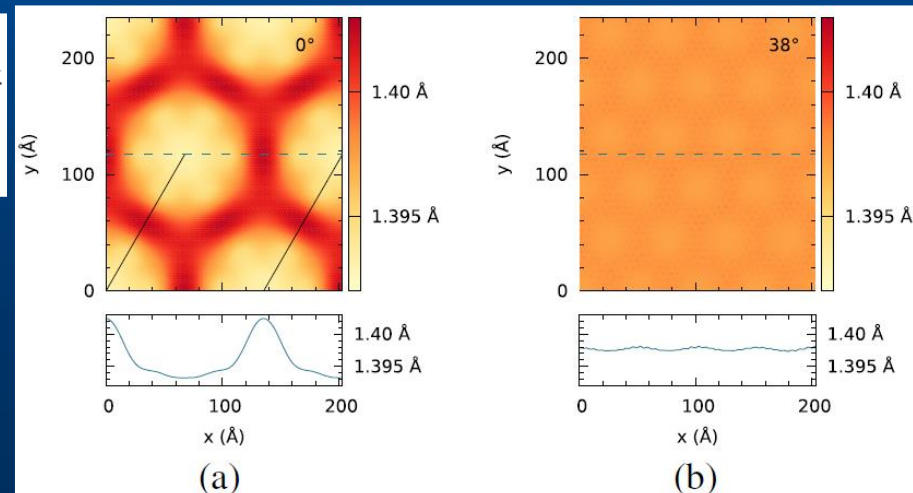
PHYSICAL REVIEW LETTERS

week ending
26 SEPTEMBER 2014

Moiré Patterns as a Probe of Interplanar Interactions for Graphene on h-BN

M. M. van Wijk, A. Schuring, M. I. Katsnelson, and A. Fasolino*

Distribution of bond length in commensurate (left) and incommensurate (right) regimes



Linear dispersion modes

T. Tudorovskiy & MIK, Phys. Rev. B **86**, 045419 (2012)

Straight zero-mass line ($y=0$)

$$\hat{H} = \sigma_x \hat{p}_x + \sigma_y \hat{p}_y + \sigma_z m(y)$$

Try the solution

$$\Psi = e^{ip_x x} \chi(y)$$

$$\chi = \frac{1}{\sqrt{2}} \begin{pmatrix} 1 \\ 1 \end{pmatrix} \eta_1 + \frac{1}{\sqrt{2}} \begin{pmatrix} 1 \\ -1 \end{pmatrix} \eta_2$$

$$\begin{pmatrix} p_x - E & \partial_y + m \\ \partial_y - m & p_x + E \end{pmatrix} \begin{pmatrix} \eta_1 \\ \eta_2 \end{pmatrix} = 0$$

Linear-dispersion mode
(LDM)

$$E = -p_x$$

$$\eta_1 = 0$$

$$\eta_2(y) = \exp \left[- \int_0^y dy' m(y') \right]$$

Allowed if m is positive for positive y and negative for negative y

Well known “zero modes” in 1D (supersymmetric QM, fractional charge and solitons in polyacetylene, etc).

Tunneling between zero-mass lines

LDM as models for counterpropagating edge states in TI, QHE, SQHE...

$$m(y) = y^2 - a^2$$

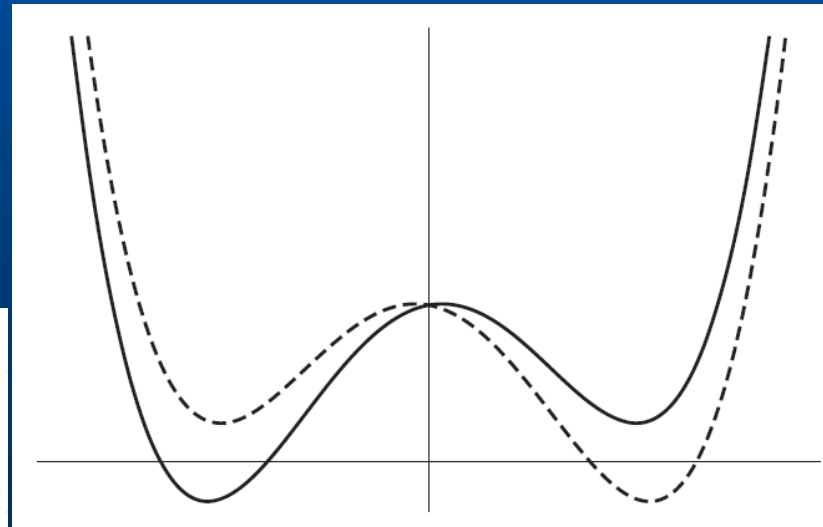
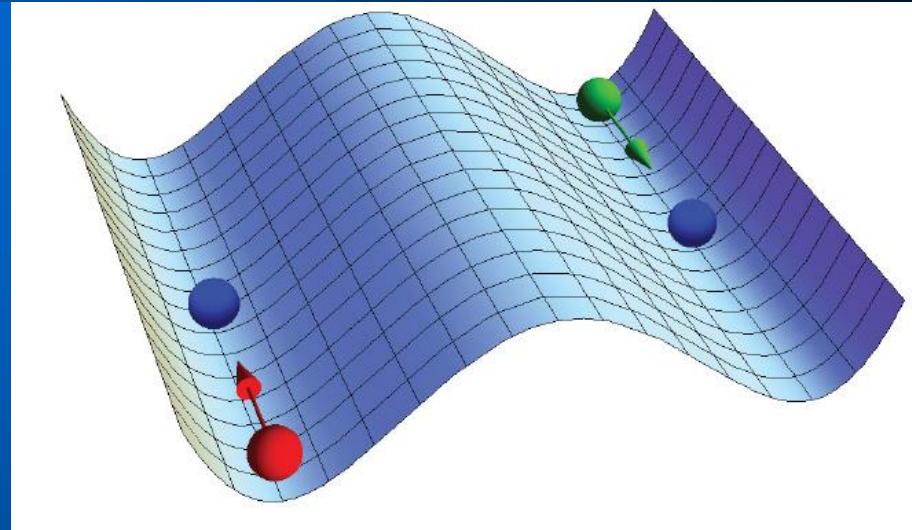
$$[-\partial_y^2 + m(y)^2 + m'(y)]\eta_1 = \lambda\eta_1$$

$$[-\partial_y^2 + m(y)^2 - m'(y)]\eta_2 = \lambda\eta_2$$

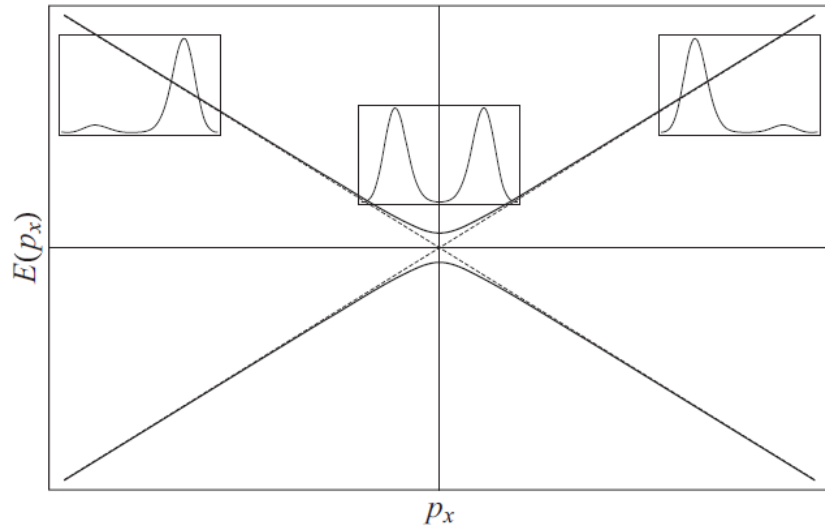
Effective potentials

$$v_1(y) = m(y)^2 + m'(y) = (y^2 - a^2)^2 + 2y$$

$$v_2(y) = m(y)^2 - m'(y) = (y^2 - a^2)^2 - 2y$$



Tunneling between zero-mass lines II



Tunneling splitting

$$2|p_y| = 2\sqrt{\frac{a}{\pi}} \exp(-4a^3/3)$$

General case, ZML at $y = a_1, a_2$

proportional to $\exp \left[- \int_{a_1}^{a_2} |m(y)| dy \right]$

It does not matter whether $m(y)$ is symmetric or not – you always have a tunneling (in contrast with the standard two-well problem), due to existence of zero mode for any $m(y)$, $p_x=0$ (supersymmetry)

Tunneling between edges determines accuracy of quantization in QHE (QSHE) in ideal situation (zero temperature, etc.)

Bent zero-mass line

Parametrization of the line

$$\{x, y\} = \mathbf{R}(\tau)$$

$$|\mathbf{R}'(\tau)| = 1$$

New variables near the line

$$\{x, y\} = \mathbf{R}(\tau) + \xi \mathbf{n}(\tau)$$

τ - coordinate along the line, ξ - normal to the line

Jacobian

$$J = \frac{D(x, y)}{D(\tau, \xi)} = 1 - k(\tau)\xi$$

k - curvature

$$\tilde{\Psi} = \sqrt{1 - k(\tau)\xi} \Psi$$

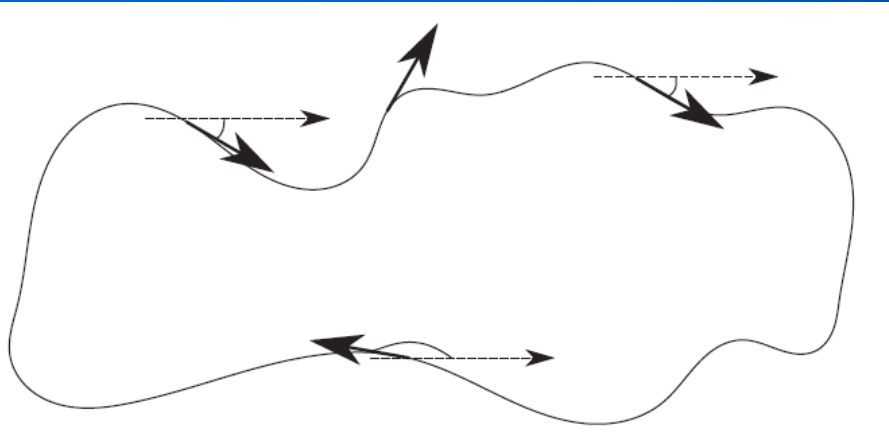
$$\int_V d\tau d\xi (\tilde{\Psi}^\dagger \tilde{\Psi}) = 1$$

$$\hat{H} \tilde{\Psi} = E \tilde{\Psi}$$

The new Hamiltonian
(exact)

$$\begin{aligned} \hat{H} = & \frac{\sigma \mathbf{R}'(\tau)}{1 - \xi k(\tau)} \hat{p}_\tau - i \sigma \mathbf{n}(\tau) \frac{\partial}{\partial \xi} + \sigma_z m \\ & - \frac{ik \sigma \mathbf{n}(\tau)}{2[1 - \xi k(\tau)]} - \frac{i \sigma \mathbf{R}'(\tau) \xi k'(\tau)}{2[1 - \xi k(\tau)]^2} \end{aligned}$$

Bent zero-mass line II



Smooth line: $|m'_\tau| \ll |m'_\xi|$

$$\hat{H} \simeq \hat{H}_0 + \hat{H}_1$$

$$\begin{aligned}\hat{H}_0 &= \sigma \mathbf{R}'(\tau) \hat{p}_\tau - i \sigma \mathbf{n}(\tau) \frac{\partial}{\partial \xi} + \sigma_z m, \\ \hat{H}_1 &= \sigma \mathbf{R}'(\tau) \xi k(\tau) \hat{p}_\tau - \frac{ik}{2} \sigma \mathbf{n}(\tau).\end{aligned}$$

We use adiabatic approximation and construct semiclassics

Symbol of the operator
in adiabatic approximation

$$\begin{aligned}\left[\sigma \mathbf{R}'(\tau) p_\tau - i \sigma \mathbf{n}(\tau) \frac{\partial}{\partial \xi} + \sigma_z m \right] \chi(p_\tau, \tau) \\ = L_0(p_\tau, \tau) \chi(p_\tau, \tau).\end{aligned}$$

Quantization rule for the bent line

Quantization condition
 n integer, w winding #

$$\frac{1}{2\pi} \oint p_\tau d\tau - \frac{E}{2\pi} \oint \langle \tilde{\chi}_1 \xi \chi_2 \rangle_\xi k(\tau) d\tau = n - \frac{w}{2}$$

$$p_\tau = \pm \sqrt{E^2 - \lambda(\tau)}, \quad \lambda(\tau) = L_0^2(p_\tau = 0, \tau).$$

The linear dispersion mode, line length l

$$E_n = -\frac{2\pi}{l} \left(n - \frac{w}{2} \right) + \frac{2\pi n}{l^2} \oint \langle \tilde{\chi}_1 \xi \chi_2 \rangle_\xi k(\tau) d\tau$$

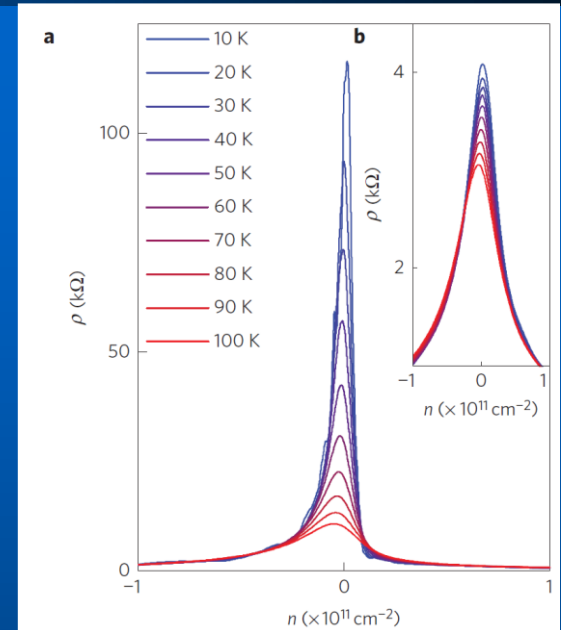
$$\langle \tilde{\chi}_1 \xi \chi_2 \rangle_\xi = -\frac{N^2(\tau)}{2} \int_{-\infty}^{\infty} \xi \exp \left[-2 \int_0^\xi d\xi' m(\tau, \xi') \right] d\xi$$

$$N(\tau) = \left\{ \int_{-\infty}^{\infty} \exp \left[-2 \int_0^\xi d\xi' m(\tau, \xi') \right] d\xi \right\}^{-1/2}$$

Consequences for electronic transport

In commensurate phase average gap is non zero,
and system can be insulating

For incommensurate phase, the average gap is zero,
and there are electron states along zero-mass lines



Woods et al, Nature Phys. 10, 451
(2014)

Model of percolation along zero-mass lines

Classical model is correct if the moiré period is larger than $\hbar v/\Delta$ (in reality, this parameter is not very large but acceptable)

Consequences for electronic transport II

PRL 113, 096801 (2014)

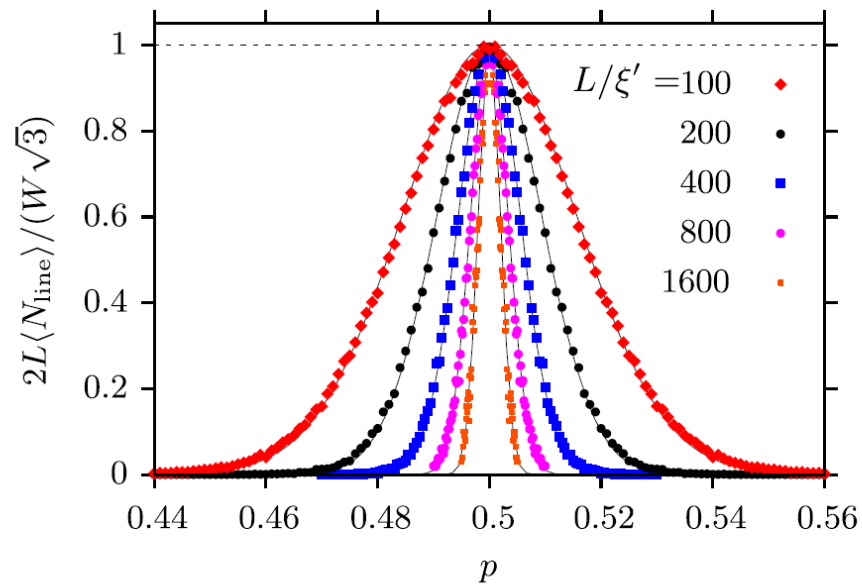
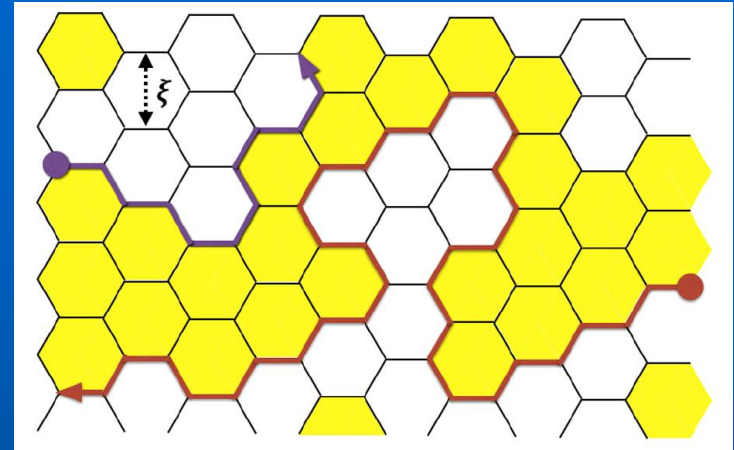
PHYSICAL REVIEW LETTERS

week ending
29 AUGUST 2014

Metal-Insulator Transition in Graphene on Boron Nitride

M. Titov and M. I. Katsnelson

2D percolation: mathematically rigorous theory exists (Smirnov)



$$\langle N_{\text{line}} \rangle = \frac{\sqrt{3}W}{2L} \exp \left[-\frac{(p - 1/2)^2}{p_0^2} \right], \quad (4)$$

where $p_0 = c(\xi'/L)^{3/4}$ with $c \approx 0.7$ (see Fig. 3).

Critical percolation cluster is
“thick” and fractal

FIG. 3 (color online). The average number of zero-mode lines connecting the leads at $x = 0$ and $x = L$ in the random walk model on a hexagonal lattice (see Fig. 2) with periodic boundary conditions in y . The dots represent numerical data obtained for $W/L = 2$. Solid lines correspond to Eq. (4).

Consequences for electronic transport III

Landauer formula for conductance

$$G = \frac{2e^2}{h} \langle N_{line} \rangle$$

Exact result for 2D percolation (Cardy)

$$\langle N_{line} \rangle = \frac{\sqrt{3}}{2} \frac{L_x}{L_y}$$

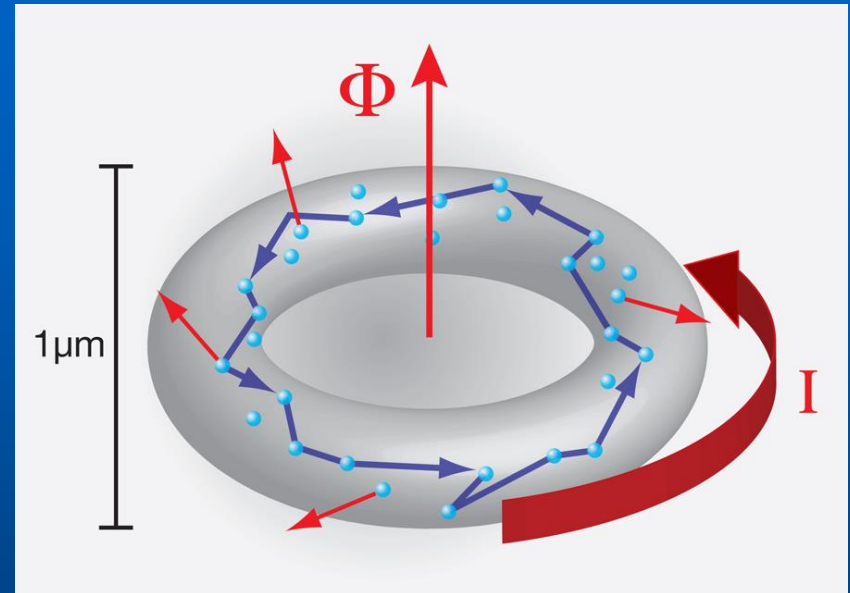
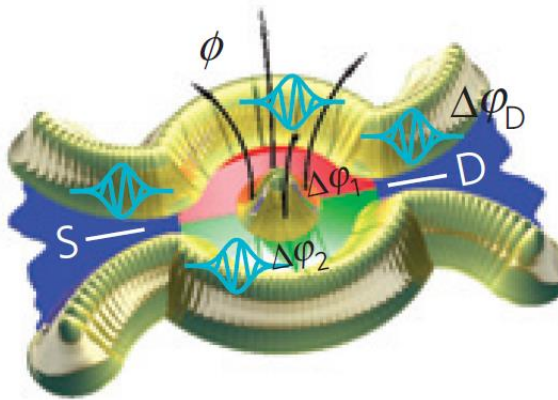
Exact minimal conductivity
in percolation model

$$\sigma = \sqrt{3} \frac{e^2}{h}$$

Aharonov-Bohm effect and spectral flow

Persistent current in a ring

$$\Delta\varphi_D = \frac{\phi}{\phi_0} 2\pi$$



If the flux through the ring is integer (in units of flux quantum) the spectrum returns to the initial point

Timur Tudorovskiy^{*,1}, Vladimir E. Nazaikinskii^{2,3}, and Mikhail I. Katsnelson¹

Spectral flow for Aharonov–Bohm rings generated by zero-mass lines

Phys. Status Solidi RRL 7, No. 1–2, 157–159 (2013)

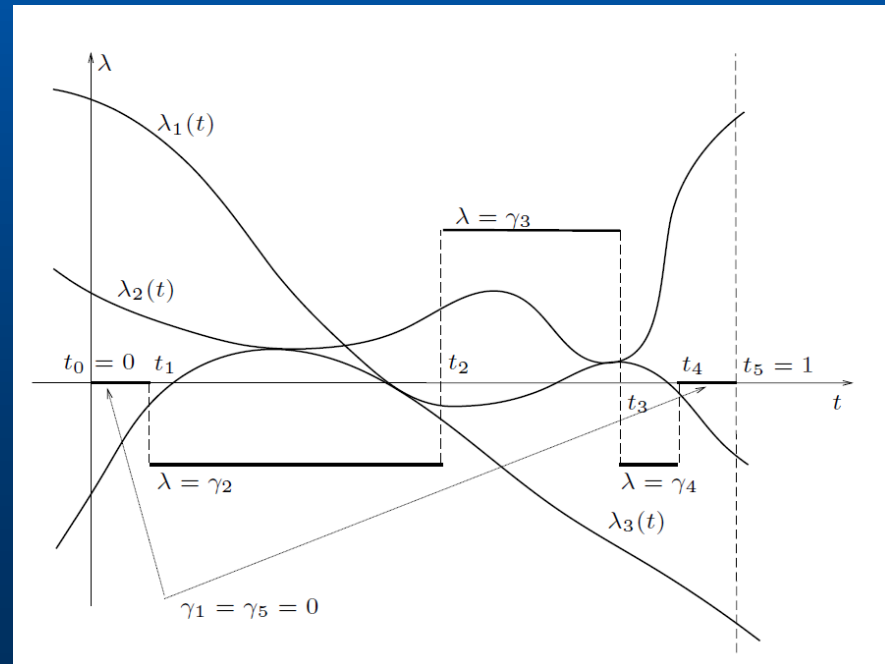
Aharonov-Bohm effect and spectral flow II

Dirac fermions: does coincidence of the spectrum means coincidence of each eigenvalue separately?

No, if the spectrum is from $-\infty$ to $+\infty$ (e.g., $n \rightarrow n+1$, n integer)
For Dirac fermions – the situation may be nontrivial!!!

$$\text{sf}\{B_t\} = \sum_{j=1}^n m_j \text{sign}(\gamma_j - \gamma_{j+1})$$

of eigenvalues crossing some value from below to above minus
of eigenvalues crossing some value from above to below



Aharonov-Bohm effect for zero-mass loop

Add vector potential

$$\hat{H} = -\frac{i\boldsymbol{\sigma}\mathbf{R}'(\tau)}{\sqrt{1-\xi k(\tau)}} \frac{\partial}{\partial \tau} \frac{1}{\sqrt{1-\xi k(\tau)}} - i\boldsymbol{\sigma}\mathbf{n}(\tau) \frac{\partial}{\partial \xi} \\ - \frac{ik\boldsymbol{\sigma}\mathbf{n}(\tau)}{2(1-\xi k(\tau))} - \boldsymbol{\sigma}\mathbf{A} + \sigma_z m .$$

Quantization condition

$$E \left(l + \oint G(\tau) k(\tau) d\tau \right) \\ = 2\pi \left(n + \frac{1}{2} \right) + B \left(S + \oint G(\tau) d\tau \right)$$

Magnetic flux

$$\Phi = B \left(S + \oint G(\tau) d\tau \right)$$

$$G(\tau) := 2\langle \tilde{\chi}_{01} \xi \chi_{02} \rangle_{\xi}$$

$El = 2\pi(n + 1/2) + \Phi + \dots$ When flux grows it works like $n \rightarrow n+1$

Aharonov-Bohm effect and spectral flow in graphene rings

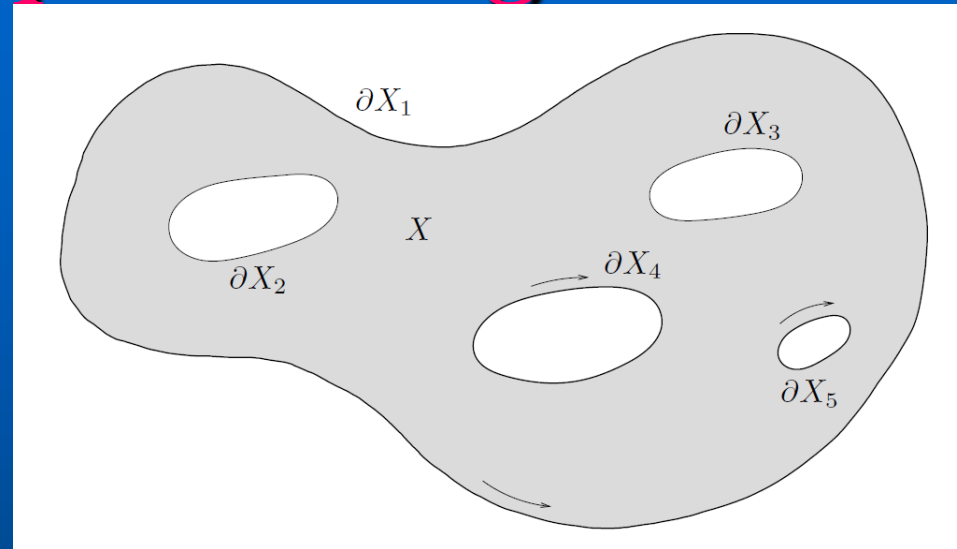
Consequences of non-zero spectral flow: positron (hole) states will move to electron region (or vice versa) – creation of e-h pairs from vacuum by adiabatically slow increasing magnetic field

At any Fermi energy, at some flux, one of eigenvalues will coincide with the Fermi energy – many-body instabilities, etc.

Conditions of nonzero spectral flow for massless Dirac fermions (M. Prokhorova 2011, MIK & V. Nazaikinskii 2012): depend on boundary conditions

Aharonov-Bohm effect and spectral flow in graphene rings II

Geometry of the sample

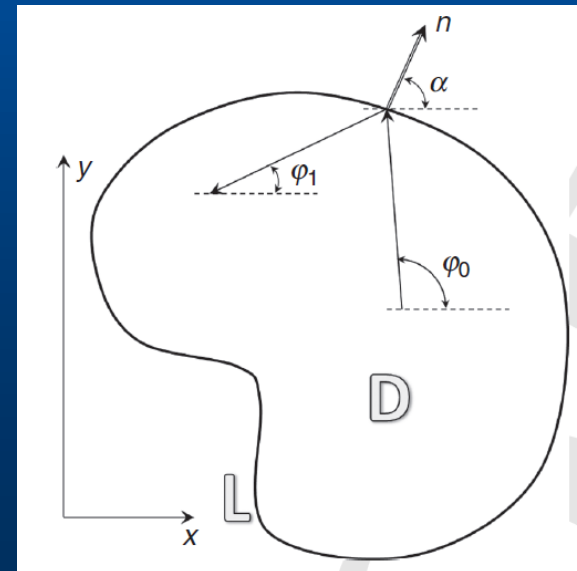


Berry-Mondragon boundary condition

$$\frac{\psi_2}{\psi_1} = iB \exp(i\alpha(s))$$

(mass opening at the Boundary)

B is nonzero real number



Aharonov-Bohm effect and spectral flow in graphene rings III

“gauge transformation” $D_0 \rightarrow \mu D_0 \mu^{-1}$

Theorem 1. *The spectral flow of the family (2) is given by the formula*

$$\text{sf } D_t = \text{wind}_{\partial^+ X} \mu, \quad (3)$$

where $\partial^+ X$ is the part of ∂X where $B > 0$ and

$$\text{wind}_{\partial^+ X} \mu = \frac{1}{2\pi i} \oint_{\partial^+ X} \frac{d\mu}{\mu}$$

is the winding number of the restriction of the function μ to $\partial^+ X$. (The set $\partial^+ X$ is a union of finitely many circles; when defining the winding number, the positive sense of any of these circles is the one for which the domain X remains to the left when moving along the circle.)

Spectral flow = number of fluxes through the holes with positive B (flux through the external boundary is taken with the opposite sign)

Aharonov-Bohm effect and spectral flow in graphene rings IV

The way of realization: ring with opposite signs of masses at inner and outer boundaries (chemically functionalized graphene; quantum wells CdTe/HgTe/CdTe with varying width; magnetic spots with different signs of magnetization at the surface of 3D topological insulator)... and you will see vacuum reconstruction and other nice stuff

In graphene: valley polarization (electrons \rightarrow holes in valley K and holes \rightarrow electrons for valley K')

Partial Spectral Flow

Eur. Phys. J. C (2020) 80:888
<https://doi.org/10.1140/epjc/s10052-020-08464-z>

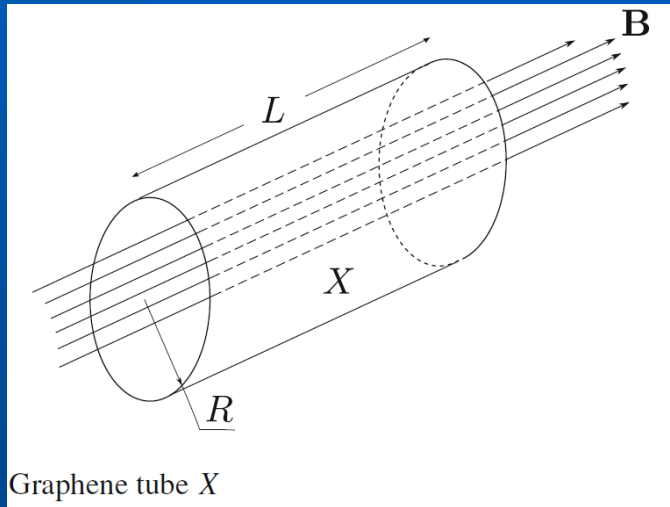
THE EUROPEAN
 PHYSICAL JOURNAL C



Regular Article - Theoretical Physics

Partial spectral flow and the Aharonov–Bohm effect in graphene

Mikhail I. Katsnelson^{1,a}, Vladimir Nazaikinskii^{2,3,b}



For nonzero SF the spectrum should be unbound from both sides – impossible in real solids!

Instead of Dirac operator we consider the finite-difference Hamiltonian at honeycomb lattice

$$[\hat{H}\psi](x) = \gamma_0 \sum_y \psi(y)$$

$$\hat{H} = H(\hat{p}), \quad H(p) = \gamma_0 \begin{pmatrix} 0 & T(p) \\ T^*(p) & 0 \end{pmatrix}$$

$$T(p) = \sum_{j=1}^3 e^{i\langle \delta_j, p \rangle},$$

Partial Spectral Flow II

Eigenfunctions of the Hamiltonian is separated into two classes: “living” in the vicinity of point K and “living” in the vicinity of point K' (in some formal sense, via projectors etc.)

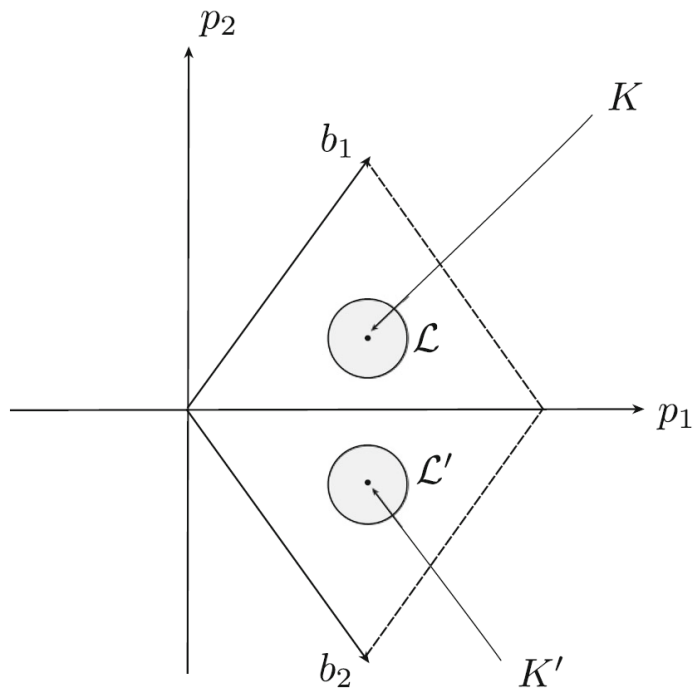


Fig. 7 Domains in the momentum space corresponding to the subspaces \mathcal{L} and \mathcal{L}' (shown by dashed disks)

Theorem 2 *There exists a $d > 0$ (which may depend on the family $\mathbf{B}(t)$) such that, for all sufficiently small $a > 0$, the family \hat{H}_t is \mathcal{L} -, \mathcal{L}' -, and $(\mathcal{L} \oplus \mathcal{L}')$ -tame, and*

$$\text{sf}_{\mathcal{L}}\{\hat{H}_t\} = \text{sf}\{\hat{D}_t\}, \quad \text{sf}_{\mathcal{L}'}\{\hat{H}_t\} = \text{sf}\{\hat{D}'_t\}, \\ \text{sf}_{(\mathcal{L} \oplus \mathcal{L}')^\perp}\{\hat{H}_t\} = 0.$$

$$\text{sf}\{\hat{D}'_t\} = -\text{sf}\{\hat{D}_t\}$$

the spectral flows of the corresponding Dirac operators

Partial Spectral Flow III

Physical picture: when flux is adiabatically changing, some hole states near K point go up and simultaneously electron states near K' points go down, that is, spontaneous formation of electron-hole pairs from different valleys

Despite total spectral flow is zero, all physical conclusions remain the same

Important: we deal with continuous models in quantum field theory but what if they are limits of some lattice theories? Topology is totally different! – But some concepts have analogs!

Conclusions

Graphene is a playground for topology and geometry

Two-dimensional gas of massless Dirac fermions in graphene

K. S. Novoselov¹, A. K. Geim¹, S. V. Morozov², D. Jiang¹, M. I. Katsnelson³, I. V. Grigorieva¹, S. V. Dubonos² & A. A. Firsov²

Vol 438|10 November 2005|doi:10.1038/nature

The half-integer QHE in graphene has recently been suggested by two theory groups^{15,16}, stimulated by our work on thin graphite films⁷ but unaware of the present experiment. The effect is single-particle and is intimately related to subtle properties of massless Dirac fermions, in particular to the existence of both electron-like and hole-like Landau states at exactly zero energy^{14–17}. The latter can be viewed as a direct consequence of the Atiyah–Singer index theorem

More than 22,000 citations (Google Scholar, Oct. 2021)

(probably more attention to this theorem than in the whole mathematics?!)

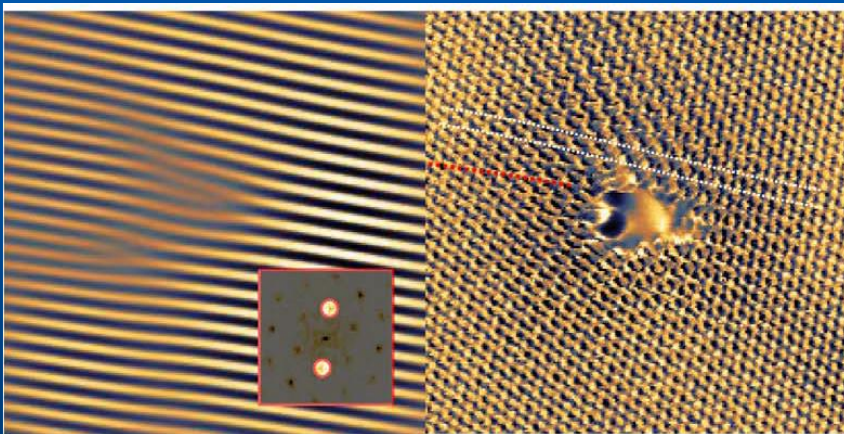
What is beyond the talk

Measuring the Berry phase of graphene from wavefront dislocations in Friedel oscillations

C. Dutreix^{1*}, H. González-Herrero^{2,3}, I. Brihuega^{2,3,4}, M. I. Katsnelson⁵, C. Chapelier⁶ & V. T. Renard^{6*}

10 OCTOBER 2019 | VOL 574 | NATURE | 219

Direct visualization of Berry phase and winding number for electron wave functions in graphene without magnetic field



Via wave-train dislocations in charge
Distributions of electrons around
H adatom (measured by STM)

M. Berry discovered the wave-train dislocations and claim
that they cannot be observed in quantum systems...

Graphene is still alive, also for mathematical physics